Dopant atom clustering and charge screening induced roughness of electronic interfaces in GaAs *p-n* multilayers

N. D. Jäger,[1] K. Urban,[1] E. R. Weber,[2] and Ph. Ebert[1,*]
[1]*Institut für Festkörperforschung, Forschungszentrum Jülich, 52425 Jülich, GmbH, Germany* [2]
Dept. of Materials Science,
University of California, and Materials Science Division, Lawrence National Berkeley Laboratory, Berkeley, California 94720
(Received 19 February 2002; published 24 May 2002)

The roughness of the *electronic* interfaces of *p-n* GaAs multilayers is investigated by cross-sectional scanning tunneling microscopy. Two physically different contributions to the roughness are found, both much larger than the underlying atomically sharp ''metallurgical'' interface. The roughness arises from the individual electrostatic screening fields around each dopant atom near the interface and from a clustering of dopant atoms. The latter leads to charge-carrier-depleted zones extending locally through the entire nominally homogeneously doped layer for layer thicknesses close to the cluster dimension, hence limiting the precision of the spatial and energetic positioning of the Fermi energy in nanoscale semiconductor structures.

DOI: 10.1103/PhysRevB.65.235302 PACS number(s): 73.20.−r, 68.35.Ct, 68.37.Ef

The functionality of semiconductor devices depends critically on the ability to spatially control the energetic position of the Fermi energy with high precision. This is frequently accomplished by a suitable incorporation of proper dopant atoms yielding the desired differently doped layers or sections in the device structure. With continuing miniaturization, however, the interfaces (and their roughness) between these differently doped areas will eventually govern the device properties once nanometer dimensions are reached. Particularly decisive will be the ''electronic'' interfaces defined by the position of the Fermi energy and not the underlying ''metallurgical'' interfaces, where the dopants change.

The direct imaging and quantitative investigation of such electronic interfaces, however, turned out to be a difficult task: Using electron holography it has been possible to probe the electrostatic potential variation between *p*- and *n*-doped layers,[1–3] but extracting quantitative values is still a hurdle and the resolution is limited to 10 nm. Therefore, it is not possible to distinguish the effects of dopant diffusion, dopant cross incorporation, or the spatial distribution of dopants, nor can the properties of the electronic interface be directly correlated with the dopants, all of which are crucial physical ingredients of a further miniaturization of devices. Other techniques, such as secondary-ion-mass spectroscopy or scanning capacitance microscopy,[4] did not solve these particular limitations either. In order to extract the physics governing the electronic interfaces between differently doped layers, one needs to be able to probe with *atomic resolution* the *individual* dopant atoms as well as electronic and geometric properties of the semiconductor structures simultaneously. In principle this can be achieved by using cross-sectional scanning tunneling microscopy (STM), which can image individual dopant atoms[5] as well as interfaces.[6] However, electronic interfaces and the correlation of their properties with dopant atoms have not been addressed yet.

In this paper we demonstrate a successful atomically resolved *electronic* interface identification, roughness mapping, correlation with the local dopant atom distribution, and association with local Fermi energy positions by investigating GaAs *p-n* multilayers using cross-sectional scanning tunneling microscopy and spectroscopy. We find that the electronic *p-n* interface exhibits a much larger roughness than the underlying essentially perfect metallurgical interface, due to long-range electrostatic screening effects of individual dopant atoms near the interface and due to a clustering of dopant atoms. The clustering and the inherently connected local lack of dopant atoms give rise to charge-carrier depletion zones extending locally through entire nominally homogeneously doped layers once their thickness is close to the cluster dimensions.

We investigated a model structure consisting of molecular beam epitaxy grown *p-n* GaAs(001) multilayers, each with a nominal thickness of 30 nm and dopant atom concentrations of $(5\pm1)\times10^{18}$ and $(4\pm1)\times10^{18}$ cm^{-3} for carbon and silicon, respectively. We cleaved these samples in ultrahigh vacuum (1×10^{-8} Pa) along a {110} plane, exposing a cross-sectional view of the multilayer structure on the cleavage surface. This cross section has been directly imaged by scanning tunneling microscopy without breaking the vacuum.

Figure 1(a) shows a large-scale cross-sectional STM overview of several *p*- and *n*-doped layers. An atomically resolved image is shown in Fig. 1(b). There are several features visible in the STM images: First, the four bright lines in Fig. 1(a) marked by black arrows are monoatomic high steps arising from the cleavage of the samples. They are not of interest here. Second, the *p*- and *n*-doped layers are separated by lines with a darker contrast, whereas the doped layers themselves have both a brighter contrast. Under the particular tunneling conditions used, the contrast of the *p*-doped layers is slightly brighter than the contrast of the *n*-doped layers. We achieved an unambiguous identification of the *n*- and *p*-doped layers on basis of the growth sequence, complementary secondary ion mass spectra, and tunneling spectra exhibiting the typical *p*- and *n*-type characteristics (see the open symbols in Fig. 2).[7]

At this stage we focus on the dark lines between the *p*-and *n*-doped layers. Tunneling spectra measured above the dark lines (filled circles in Fig. 2) show an apparently widened band gap, characteristic for a carrier depletion.[7] Thus the dark lines are the image of the depletion zones localized at *p-n* interfaces in agreement with Refs. 7 and 8. The darker contrast arises from the increased tip-induced band bending

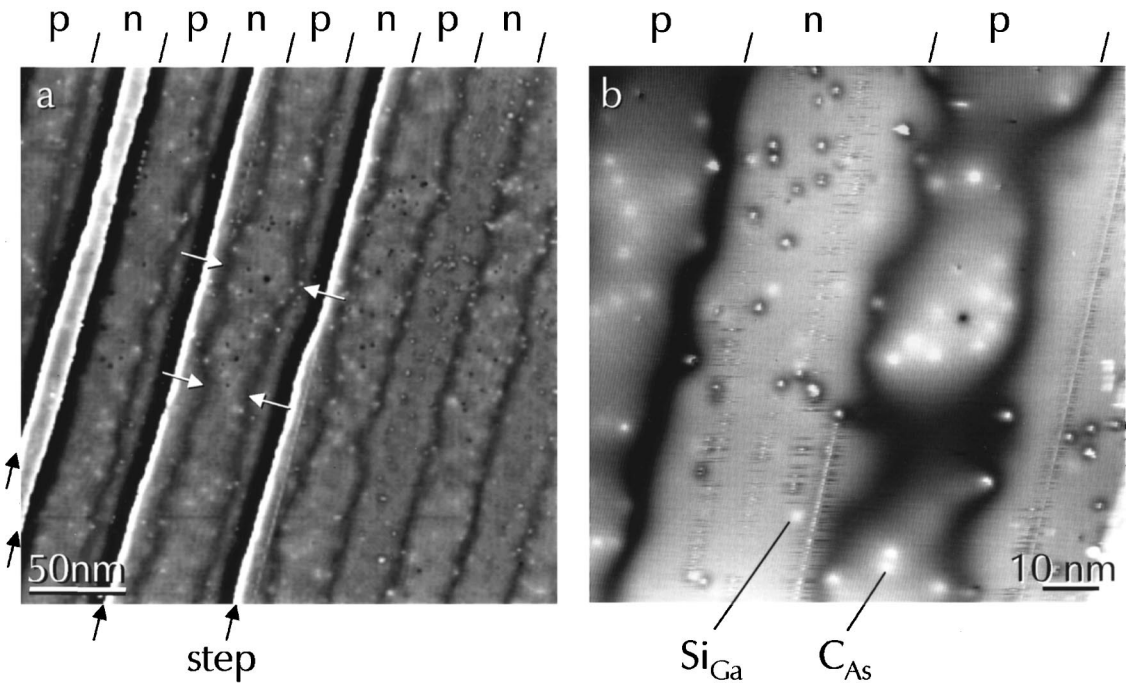

FIG. 1. Large scale (a) and atomically resolved (b) cross-sectional scanning tunneling microscopy images of multiple *p*- and *n*-doped GaAs layers marked *p* and *n*, respectively. The growth direction is from left to right. The bright lines marked by black arrows in frame (a) are monoatomic steps. The height difference between the terraces has been removed by a high pass filter. The bright hillocks marked by Si_{Ga} and C_{As} arise from individual dopant atoms. The dark lines between the *p*- and *n*-type layers are the signatures of the depletion zone at each *p*-*n* interface, and show the position of the electronic interface. Note its pronounced roughness and its correlation with the dopant atoms. All the contrast visible (except the steps) is electronic and *not* due to geometric deformations of the surface. Both images were acquired at −2 V tunneling voltage and 0.1 nA current, and show the occupied density of states.

due to the reduced charge-carrier concentration in the depletion zone.[9] The depletion zone marks the transition of the Fermi energy from close to the valence-band edge in *p*-type material to close to the conduction-band edge in *n*-doped material. Therefore, we define the electronic interface between *p*- and *n*-doped layers as the plane where the Fermi energy is at midgap position. The center of the dark lines in Fig. 1 corresponds to the spatial position of this electronic interface, which is not identical with the metallurgical interface (indicated by dashes in Fig. 1), where the doping changes from C_{As} to Si_{Ga}, or vice versa.

In fact the metallurgical interface can be directly seen in Fig. 1, because the individual bright hillocks with about 3 to 5 nm diameter, visible in *p*-doped layers as well as *n*-doped layers, are the signatures of negatively charged C_{As} and positively charged Si_{Ga} dopant atoms, respectively.[5] Their contrast is given by the image of the screened Coulomb potential,[10] which arises from the screening of the dopant charge by free charge carriers. The atomic position of the dopant atom is in the center of the bright hillocks. Note a quantitative analysis of the dopants' positions identified in high-resolution STM images showed no evidence for intermixing or cross-incorporation pointing to a sharp metallurgical interface.

Although the metallurgical interface is in our case very sharp, the electronic interface appearing as dark lines exhibits a much larger roughness. Figure 1(b) shows that the depletion zone circumvents each individual dopant atom near

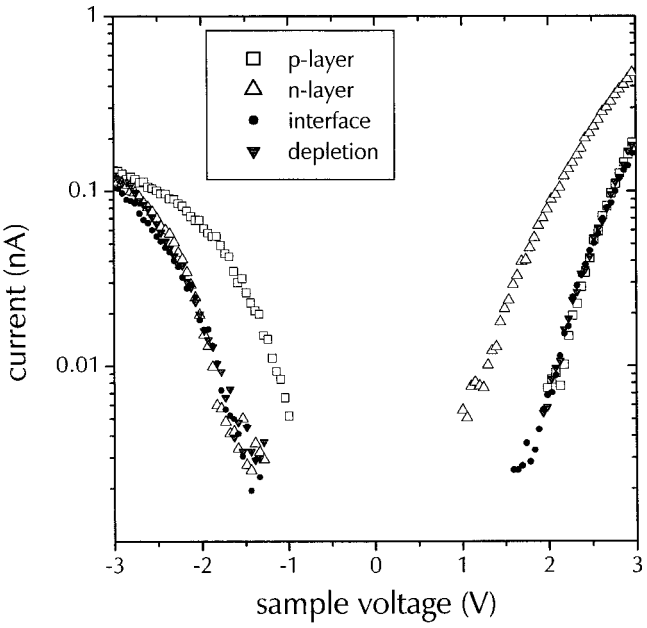

FIG. 2. Scanning tunneling current-voltage spectra acquired in the *p*-type layer (□), the *n*-type layer (△), the interface depletion zone between *p*- and *n*-type layers (●), and the depletion zone extending through the *p*-type layer due to the clustering of dopants (▼). The spectra are all corrected to a constant tip-sample distance in order to allow proper comparison.

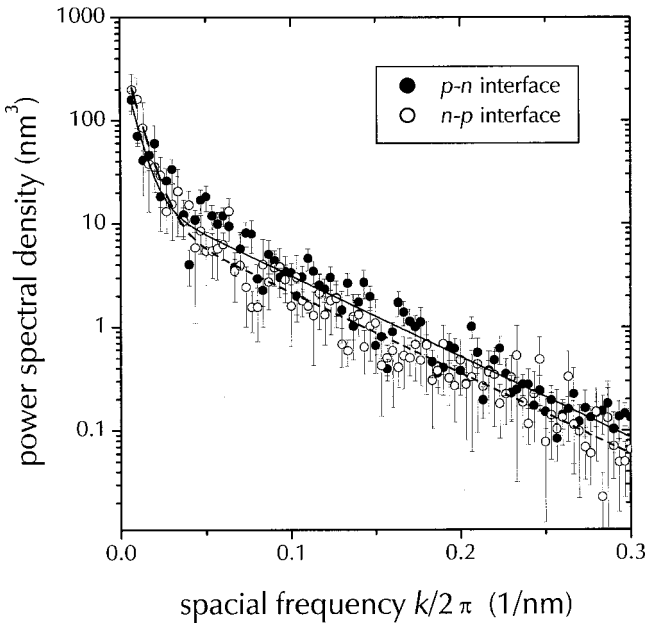

FIG. 3. Power spectral density of the electronic *p-n* (●) and *n-p* (○) GaAs interfaces obtained from STM images, as seen in Fig. 1. Each data set is fitted to a sum of two exponentials representing two scales of roughness found in each interface type. The solid (dashed) line is a fit to the data of the *p-n* (*n-p*) interface.

the interface. Undoubtedly each dopant atom near the interface causes a short range meandering of the electronic interface on the scale of 2–5 nm. A careful inspection of large scale STM images reveals a further contribution to the interface roughness on a longer length scale, leading to the electronically wide and narrow layers [see examples marked in Fig. 1(a) by white arrows].

In order to quantify the amplitude and correlation length of the two different roughness contributions, we computed the power spectral density, $\tilde{G}(k)=|\tilde{A}(k)|^2$, on basis of the deviation from mean of the interface lines $A(x)$ visible in the STM images, with $\tilde{A}(k)$ being the discrete Fourier transform of $A(x)$.[11,12] Figure 3 shows the results for the *p-n* and *n-p* interfaces. Two separate frequency ranges are visible, one at small k values with a large slope and another one at large k values with a smaller slope. We first concentrate on the latter one, which exhibits a clear exponential decay characteristic for all our interfaces. The exponential decay $\tilde{G}(k)=\pi a b^{-1} e^{-b\cdot k}$ corresponds to a Lorenzian functional dependence of the *real-space* autocorrelation function $G(x)=a/(x^2+b^2)$. Where $(a/b^2)^{0.5}$ and b are the amplitude (equivalent to root mean square roughness) and the correlation length of the interface roughness, respectively.

The entire data sets in Fig. 3 can be well described by *two* exponential decays, confirming our above observation of two different contributions to the roughness. We extracted the corresponding values for the amplitudes and the correlation lengths from the fits shown as lines in Fig. 3. For large k values the amplitudes are 1.5 ± 0.3 and 1.2 ± 0.2 nm, and the correlation lengths are 2.9 ± 0.5 and 2.9 ± 0.5 nm for the *p-n* and *n-p* interfaces, respectively. For small k values we obtained 2.2 ± 0.5 and 2.7 ± 0.4 nm as amplitudes and 26 ± 8 and 23 ± 5 nm as correlation lengths, respectively. No difference between *p-n* and *n-p* interfaces can be observed within the error margin. The excellent fit to the data can be understood in terms of a smooth meandering of the interface circumventing the dopant atoms as visible in Fig. 1(b). This is best described in real space by the above-used Lorenzian function. We emphasize that the roughness amplitudes and correlation length obtained here for the doping interfaces are about one order of magnitude larger than those typically found for heterojunction interfaces consisting of different compounds,[11,13,14] because the latter probe primarily the metallurgical interface. Furthermore, the functional dependence found in Fig. 3 differs from those found for heterojunction interfaces consisting of different compounds.[11,13,15] This again is due to the different physical origin of the interfaces (electronic versus metallurgical).

At this stage we discuss the origin of the two contributions to the roughness of the electronic interface. First, the STM images show that the roughness with correlation lengths of about 3 nm and amplitudes of about 1.5 nm can be correlated to the meandering of the electronic interface around the *individual* dopant atoms. Note that the meandering is on the same scale as the spatial extension of the charge screening clouds around each individual dopant atoms (the bright area of each dopant atom). This suggests that the screening length of the screened Coulomb potential around the individual charged dopants governs the roughness. The screening length at room temperature for doping levels close to 5×10^{18} cm^{-3} is about 1.5 nm.[16,17] This is in good agreement with the roughness values, and corroborates the importance of the charge screening in the meandering of the electronic interface at short distances.

Second, the physical origin of the long range contribution to the roughness can be perhaps best discussed using Fig. 1(b). The STM image shows that the dopant atoms within the nominally homogeneously doped layers exhibit large variations in concentration. In this particular image one can observe a cluster of C_{As} dopant atoms. Above and below are areas locally free of dopant atoms. Consequently the clustering is the origin of the long-range roughness of the interfaces with a correlation length of 25 nm and an amplitude of 2.5 nm.

The clustering affects also the electronic properties. The example of Fig. 1(b) shows that the presence of the dopant cluster locally enlarges the electronic *p*-type layer, whereas the lack of dopant atoms nearby leads to a completely depleted zone extending locally through the entire *p*-type layer. The spectrum shown as solid triangles in Fig. 2 show that these areas indeed exhibit a full depletion identical to that of the depletion zone at the *p-n* interfaces. Thus the Fermi energy is near midgap and not near the valence-band maximum as intended. Clearly the clustering of the dopant atoms causes the Fermi energy to vary strongly within the nominally homogeneously doped layers.

In conclusion, we presented a methodology to identify and investigate electronic interfaces with atomic resolution and correlate their properties with individual dopant atoms. Electronic interfaces between *p*- and *n*-doped layers in GaAs

exhibit a very large roughness arising from the discrete nature of the screening fields around individual dopant atoms and from the clustering of dopant atoms in nanoscale dimensions. Tied to this roughness are strong local variations of the Fermi energy. These can lead to failures of nanoscale semiconductor devices.

We thank W. K. Liu from IQE Inc. for providing the sample. Financial support from the Deutsche Forschungsgemeinschaft and the Director, Office of Science, Office of Basic Energy Sciences, of the U.S. Department of Energy under Contract No. DE-AC03-76SF00098 is gratefully acknowledged.

*Corresponding author (Email address: p.ebert@fz-juelich.de)

[1] W. D. Rau, P. Schwander, F. H. Baumann, W. Höppner, and A. Ourmazd, Phys. Rev. Lett. **82**, 2614 (1999).

[2] M. R. McCartney, D. J. Smith, R. Hull, J. C. Bean, E. Voelkl, and B. Frost, Appl. Phys. Lett. **65**, 2603 (1994).

[3] S. Frabboni, G. Matteucci, G. Pozzi, and M. Vanzi, Phys. Rev. Lett. **55**, 2196 (1985).

[4] H. Edwards, R. McGlothlin, R. San Martin, E. U. M. Gribelyuk, R. Mahaffy, C. K. Shih, R. S. List, and V. A. Ukraintsev, Appl. Phys. Lett. **72**, 698 (1998).

[5] Ph. Ebert, Surf. Sci. Rep. **33**, 121 (1999).

[6] E. T. Yu, Chem. Rev. **97**, 1017 (1997); R. M. Feenstra, Semicond. Sci. Technol. **9**, 2157 (1994).

[7] R. M. Feenstra, A. Vaterlaus, E. T. Yu, P. D. Kirchner, C. L. Lin, J. M. Woodall, and G. D. Pettit, in *Semiconductor Interfaces at the Sub-Nanometer Scale*, edited by H. W. M. Salemink and M. D. Pashley (Kluwer, Dordrecht, 1993), p. 127; R. M. Feenstra, E. T. Yu, J. M. Woodall, P. D. Kirchner, C. L. Lin, and G. D. Pettit, Appl. Phys. Lett. **61**, 795 (1992).

[8] M. L. Hildner, R. J. Phaneuf, and E. D. Williams, Appl. Phys. Lett. **72**, 3314 (1998).

[9] A. R. Smith, S. Gwo, K. Sadra, Y. C. Shih, B. G. Streetman, and C. K. Shih, J. Vac. Sci. Technol. B **12**, 2610 (1994).

[10] Si dopants in the topmost surface layers exhibit a dark ring around a bright center, whereas Si dopants in deeper subsurface layers appear only as a bright hillock.

[11] R. M. Feenstra, D. A. Collins, D. Z.-Y. Ting, M. W. Wang, and T. C. McGill, Phys. Rev. Lett. **72**, 2749 (1994).

[12] J. M. Bennett and L. Mattsson, *Introduction to Surface Roughness and Scattering* (Optical Society of America, Washington DC, 1989).

[13] J. Harper, M. Weimer, D. Zhang, C.-H. Lin, and S. S. Pei, Appl. Phys. Lett. **73**, 2805 (1998).

[14] W. Barvosa-Carter, M. E. Twigg, M. J. Yang, and L. J. Whitman, Phys. Rev. B **63**, 245311 (2001).

[15] E. F. Schubert, *Doping in III-V Semiconductors* (Cambridge University Press, Cambridge, 1993).

[16] R. B. Dingle, Philos. Mag. **46**, 831 (1955).

[17] Ph. Ebert, T. Zhang, F. Kluge, M. Simon, Z. Zhang, and K. Urban, Phys. Rev. Lett. **83**, 757 (1999).